Numerical calculation of the rotordynamic coefficients of a LOX-Turbopump Seal for the LUMEN LOX/LNG demonstrator rocket engine

Numerical calculation of the rotordynamic coefficients of a LOX-Turbopump Seal for the LUMEN LOX/LNG demonstrator rocket engine

Max Axel Müller, Tobias Traudt, Stefan Schlechtriem

German Aerospace Center (DLR), Langer Grund, 74239 Hardthausen

tobias.traudt@dlr.de

Abstract. In rocket engines seals are one of the key elements for a successful turbopump operation. They are not only responsible for reducing the leakage but they also have a huge influence on the rotordynamic behaviour. Depending on the design, the seal on a turbopump impeller can damp or excite rotordynamic instabilities. In this work we present transient 3D CFD simulations of straight gap seals, which are used to determine the rotordynamic coefficients. After that the numerical simulation is extended to characterize the influence of the impeller to housing clearance and swirl brakes on the rotor dynamic coefficients. We show that the inertia term cannot be neglected for the investigated nominal rotational speed of the rotor and high absolute whirl frequency ratios especially for the rotor housing clearance. Finally the coefficients calculated by numerical simulation are used in the equations of motion for a floating ring seal and the equations are solved numerically to do a sensitivity study of a floating ring to variations in axial force, rotor displacement and floating ring mass.

1. Introduction

The DLR is developing a modular breadboard engine called LUMEN (liquid upper stage demonstrator engine) for test bench use. LUMEN is an LOX/LNG expander cycle engine with a nominal thrust of 25kN. LUMEN will use two turbopumps which use the same underlying design to allow modularity, reusability and longevity [1].

There are many design challenges in turbopump development one of which is rotordynamics and vibrations of the turbopump components exciting shaft vibrations. If the rotor of the OTP (oxygen turbopump) comes into contact with the housing an oxygen fire will destroy the turbopump instantaneously.

There are several examples for the difficulties which can be attributed to rotordynamics. One example are the instabilities during the development of the SSME (Space Shuttle Main Engine) which took 10 months to resolve [2]. Another example is the explosion of an Antares rocket in 2014 which was caused by the rotor of the OTP coming into contact with the stationary parts in the pump [3].

In the following sections we will describe the framework which has been set up in order to investigate the rotordynamic effects of straight gap seals, rotor/housing clearances and floating ring seals. The framework is used in the development of the LUMEN turbopump impeller seals.

2. Background

The dynamic behaviour of the turbopump rotor is determined by the mass distribution and the forces acting on it during operation. Two of the forces acting on the rotor are the dynamic fluid force in the gap of the impeller seals as well as the dynamic fluid force between the impeller shroud and the housing. The seals on the impeller have therefore two functions, reducing losses by limiting seal mass flow and stabilizing the rotor by the forces introduced.

Unfortunately the fluid dynamic forces on the rotor are not always stabilizing but depending on the type of seal, the design of the impeller/housing clearance and the so called whirl frequency ratio

$$WFR = \frac{\Omega_{orb}}{\Omega_{rot}} \tag{1}$$

the forces can be either stabilizing or destabilizing. In equation 1 Ω_{rot} is the angular velocity of the shaft and Ω_{orb} is the angular velocity of the shaft orbit due to deflection by a force acting on it.

For WFR > 0 the shaft deflection is rotating in the direction of the shaft rotation and for WFR < 0 it is counter rotating.

To determine if a force is stabilizing or destabilizing we consider its tangential and radial components separately as shown in Figure 1 [4].

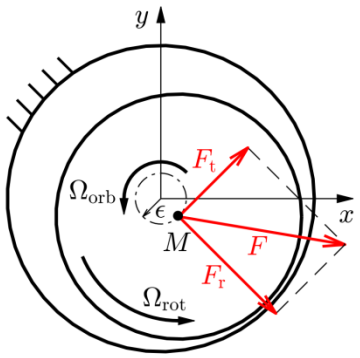

Figure 1. Components of the fluid forces

It is obvious that a positive radial force F_r will increase the radius of the shaft orbit ϵ and a negative F_r will decrease ϵ. The tangential force F_t will have a damping affect on Ω_{orb} if it is positive while WFR < 0 and it will be destabilizing if it is negative for WFR > 0 (see red areas in Figure 2).

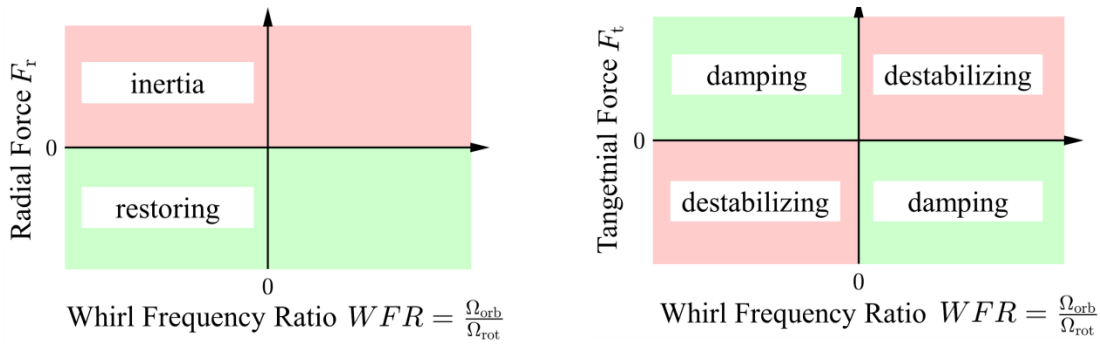

a) Influence of radial force **b)** Influence of tangential force

Figure 2. influence of fluid force components according to [4]

According to [5] and [6] the following linearized equations of motion describe the rotordynamic behaviour of straight gap seals:

$$-\begin{bmatrix} F_x \\ F_y \end{bmatrix} = \begin{bmatrix} M & M_{kk} \\ -M_{kk} & M \end{bmatrix} \begin{bmatrix} \ddot{x} \\ \ddot{y} \end{bmatrix} + \begin{bmatrix} D & D_{kk} \\ -D_{kk} & D \end{bmatrix} \begin{bmatrix} \dot{x} \\ \dot{y} \end{bmatrix} + \begin{bmatrix} K & K_{kk} \\ -K_{kk} & K \end{bmatrix} \begin{bmatrix} x \\ y \end{bmatrix} \tag{2}$$

The entries on the main diagonal of the matrices are the mass, damping and stiffness coefficients (M, D, K). They create a force in the direction of the acceleration, velocity and deflection of the rotor whereas the cross coupling coefficients (index kk) create forces perpendicular to it. It is worthwhile to note that the mass matrix acts like a kind of inertia which is an abstract representation of the fluid forces counteracting the acceleration of the rotor.

It is possible to determine the coefficients by assuming a circular orbit of the shaft and transforming the forces from their Cartesian form in equation 2 to their radial and tangential components. This results in

$$\begin{aligned} \frac{F_r}{\epsilon} &= M \cdot {\Omega^2}_{orb} - D_{kk} \cdot \Omega_{orb} - K, \\ \frac{F_t}{\epsilon} &= -M_{kk} \cdot {\Omega^2}_{orb} - D \cdot \Omega_{orb} + K_{kk}. \end{aligned} \tag{3}$$

With 3 operation points of different Ω_{orb} and known values for the radial and tangential forces as well as known rotor eccentricity the 6 components can be determined. It does not matter if the operating points are either experimental or numerical. In this work transient 3D CFD simulations with an eccentricity of 10% of the gap height will be carried out to create the database for the coefficient evaluation. In [7] simulations with eccentricities up to 40% gap height were performed and showed that the maximum error is 8.5% for the radial force compared to the values obtained at 10%. This accuracy is considered to be sufficient and the results obtained at 10% gap height will be used for eccentricities up to 30-40%.

3. Numerical setup

Figure 3 shows a cut view of the impeller with its seals in the front and back. The volume under consideration in this work is the blue area in Figure 3. The main flow exits the impeller and the secondary flow travels through the impeller/housing clearance before leaking through the impeller front seal. The clearance is considered in the simulation because it has an influence on the swirl of the flow entering the seal. Inlet swirl has a negative influence on the cross coupled stiffness according to [5], [8].

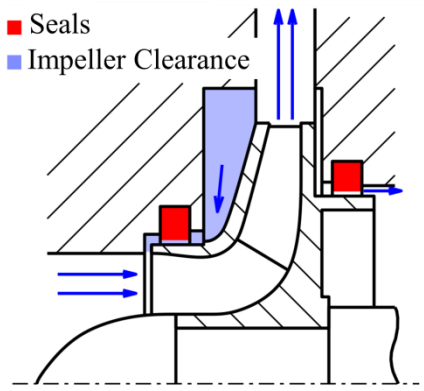

Figure 3. Impeller to housing clearance

Ansys CFX was used for all simulations [9] with the SST turbulence model. The flow solver uses all roughness values in Table 1 as equivalent sand roughness.

The discretization of the volume leads to the structured mesh in Figure 4. A convergence study has been carried out and resulted in a mesh with 1,096,000 cells for the reference geometry and a mesh with 990,000 cells for the smaller rotor to housing clearance. The meshes are similar in the seal gap with 24 cells in the radial direction. Please note that in Figure 4 the mesh is mirrored at the vertical axis compared to Figure 3 in order to have a flow from left to right.

a) 2D cut of reference geometry

b) 3D view of reference geometry

c) 3D cut of smaller rotor to housing clearance (see section 5.)

Figure 4. CFD simulation mesh

The boundary condition at the inlet to the simulation area is a mass flow with a swirl representative of the actual flow in the pump volute. The exit boundary condition is the static pressure at the impeller inlet. All boundary conditions are summarized in Table 1.

Table 1. boundary conditions for all simulations

Property	value	unit
pressure difference	76	bar
rotational speed	25200	min^{-1}
circumferential speed at inlet	67,4	m/s
seal gap length	7	mm
seal gap inner radius	29.825	mm
seal gap height	50	µm
rotor eccentricity	5	µm
roughness seal gap	1	µm
roughness impeller	10	µm

The fluid in the simulations is liquid oxygen with constant fluid properties. The properties are considered constant to simplify the simulation and speed up the calculation time. Another benefit is the prevention of cavitation in the seal gap, which might happen close to the exit and also has a negative impact on computation time. The errors introduced by this approach are expected to be of negligible order since the attribution of the exit area to the overall force on the rotor is small.

Table 2. fluid properties of liquid oxygen at p = 40bar and T = 98K

Property	value	unit
density	1111.3	kg/m^3
heat capacity	1701.3	$J/kg \cdot K$
thermal conductivity	142.68	$mW/m \cdot K$
dyn. viscosity	166.78	$\mu Pa \cdot s$

4. Reference geometry

4.1. Flow field, pressure field, leakage, swirl ratio

Figure 5 shows the pressure field and the stream lines in a side view and a cut about 0.2mm in front of the seal entrance (see dashed line in Figure 5a) of the reference geometry. Close to the shroud of the impeller the friction imposes a swirl on the flow which directs the flow radially outwards. A large eddy forms in the rotor to housing clearance which extends over the whole circumference. Due to the eddy, the stream lines going to the seal have a significant swirl which leads to a pressure gradient that decreases the inlet pressure at the seal. This is beneficial for leakage as will be shown in the following sections where the effect of a swirl brake is examined.

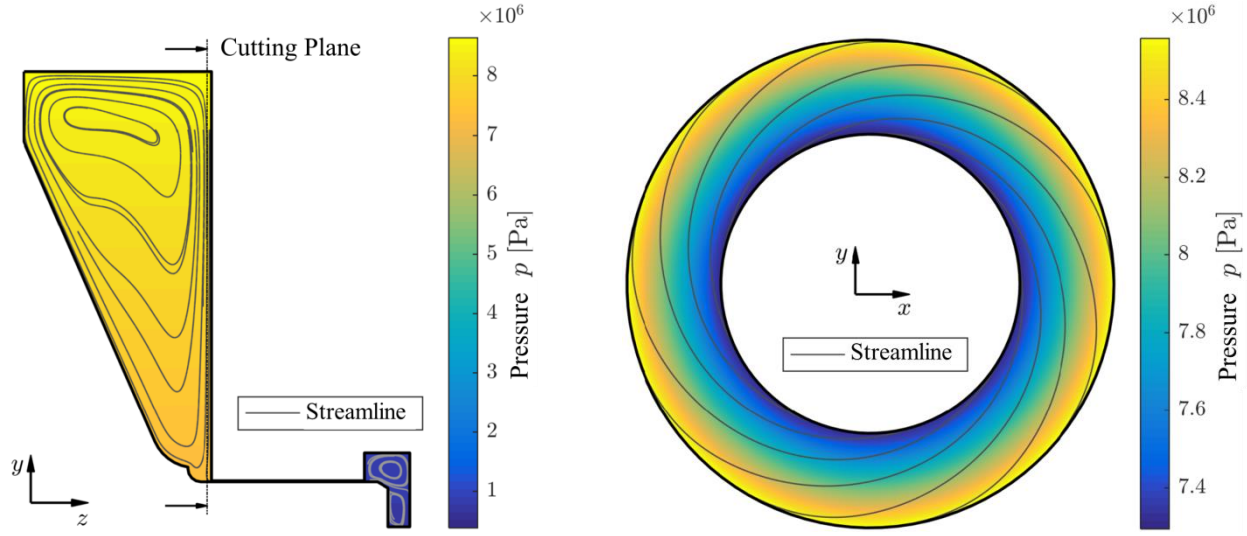

a) side view **b)** cross section

Figure 5. flow field of reference geometry

Table 3 shows the leakage and the swirl ratio for the reference geometry. The leakage mass flow for the seal is 0.4kg/s which is around 7% of the impeller mass flow.

The swirl ratio $c_{u,0}$ is defined as the ratio of the circumferential component of the fluid at the inlet $c_{u,in}$ to the circumferential speed of the rotor at the seal diameter $c_{u,rot}$

$$c_{u,0} = \frac{c_{u,in}}{c_{u,rot}}. \tag{4}$$

For the reference geometry $c_{u,0}$ is 0.45.

4.2. Rotor dynamic coefficients

To determine the rotor dynamic coefficient 7 transient simulations have been performed in a range of -1.2 < WFR < 1.2.

The results for the reference geometry are shown in red in Figure 6 for the impeller housing clearance and the seal respectively. The dashed and solid lines are curve fit of the linearized model (equation 3) as described in section 2. The rotor dynamic coefficients are summarized in Table 4.

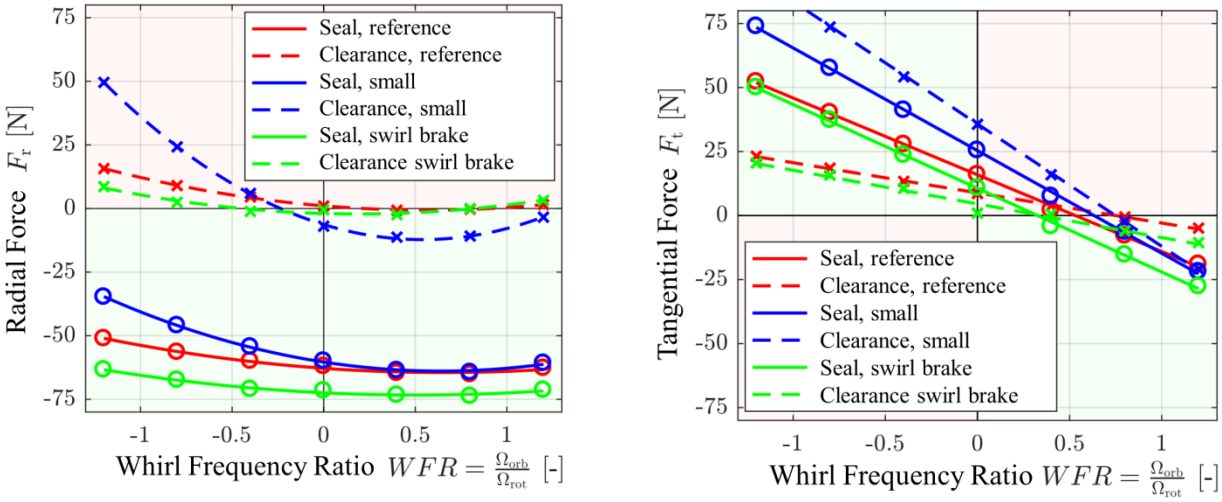

a) radial force **b)** tangential force

Figure 6. WFR dependent forces for all simulations

One can see that the linearized model predicts the forces on the rotor well. The radial force is following a quadratic function while the tangential force is following a linear function. For this reason, the cross coupled mass terms can be neglected ($M_{kk} = 0$), which is in line with literature [5].

The radial force of the seal is negative for all WFR and has a restoring effect, while the radial force of the clearance is destabilizing. Since the forces in the seal are always higher than the clearance forces the resulting force is always restoring.

The tangential forces show in both cases a small area for WFR > 0 where they act in a destabilizing way and the seal forces are, again, bigger than the clearance forces.

Table 3. leakage and swirl ratio of reference geometry and smaller clearance

property	reference	small	swirl brakes	unit
leakage	0.4	0.39	0.43	kg/s
inlet swirl ratio	0.45	0.43	0.26	-

5. Small impeller to housing clearance

To optimize the pump design a decrease of the impeller to housing clearance was designed and simulated to see its effect on the rotor dynamic coefficients. Figure 4c shows the mesh for the new simulation.

5.1. Flow field, pressure field, leakage, swirl ratio

The flow field is comparable to the reference geometry with a large eddy and a radial pressure gradient.

However, the viscous losses in the smaller clearance are higher leading to a lower inlet velocity to the seal. This leads to less leakage and a slightly lower inlet swirl ratio (see Table 3).

Table 4. rotor dynamic coefficients of the reference geometry and smaller clearance

	seal			rotor/housing clearance		
coefficient	reference	smaller clea.	swirl brakes	reference	smaller clea.	swirl brakes
M [kg]	1.125 E-1	2.479 E-1	9.776 E-2	1.507 E-1	5.866 E-1	1.534 E-1
M_{kk} [kg]	-	-	-	-	-	-
D [kg/s]	2.272 E3	3.304 E3	2.478 E3	8.929 E2	3.621 E3	9.957 E2
D_{kk} [kg/s]	3.878 E2	8.400 E2	2.633 E2	4.485 E2	1.667 E3	1.514 E2
K [kg/s²]	1.256 E7	1.207 E7	1.449 E7	-2.089 E5	1.263 E6	3.918 E5
K_{kk} [kg/s²]	3.184 E6	5.069 E6	2.130 E6	1.769 E6	7.150 E6	9.074 E5

5.2. Rotor dynamic coefficients

The radial and tangential forces of the smaller clearance are compared to the reference geometry in Figure 6 in blue. For small WFR the radial force in the seal gap is smaller than for the reference geometry. The radial force in the rotor/housing clearance is now stabilizing the rotor for WFR > 0 but the negative destabilizing force significantly increases for WFR < 0. The negative radial force even exceeds the seal force which leads to an overall destabilizing influence of the smaller clearance.

The slope of the tangential forces is steeper than in the reference case which leads to higher damping in the range of WFR < 0 and WFR >0.8 but on the other hand the destabilizing effect is more pronounced in the other areas.

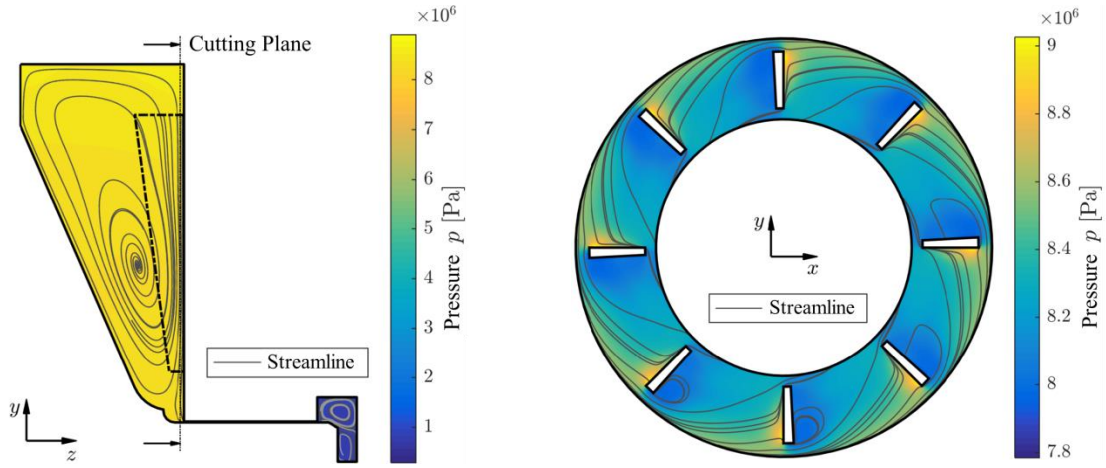

a) side view **b)** cross section

Figure 7. flow field of geometry with swirl brakes

The rotor dynamic coefficients in Table 4 reflect the behaviour described above. The non-linearity is increased by the increase of the mass coefficient and the radial forces are shifted by the change in D_{kk}. These effects might be attributed to more pronounced viscous effects which increase the friction on the impeller and to the decrease in space for the eddy which forms in the rotor to housing clearance.

For the seal, the main component of the stiffness K remains almost the same while it changes the direction and increases significantly for the smaller rotor-housing clearance. But K is still one order of magnitude smaller for the clearance than for the seal and hence of negligible influence.

6. Swirl brakes

Due to the aforementioned reasons swirl brakes in the rotor/housing clearance have been evaluated. Eight blades have been added to the housing and the flow field around them is shown in Figure 7. One can see asymmetrical flow separation on the suction side of the swirl brakes which is caused by the non-ideal inlet flow and the low number of brakes. Nevertheless the swirl is reduced by 42% (see Table 3) which also decreases the radial pressure gradient compared to Figure 5. The latter increases the pressure difference over the seal gap which in turn increases the seal leakage flow by 7.7% in comparison to the other simulations. Compared to the total pump mass flow the increase in leakage is less than 0.7%. The decrease in leakage performance is balanced by an increase in rotordynamic performance (see Figure 6 in green). The radial forces of the seal gap are the highest for all configurations because the increased axial pressure difference enhances the so called Lomakin-effect [10]. The trend of the tangential forces shows a better behaviour in the way that the range of destabilizing forces is decreased. The tangential forces damp rotor oscillations almost over the whole range of WFR.

7. Sensitivity study on floating ring seal parameters

Floating ring seals (FR) as the name implies are not fixed on the rotor. The seal ring can move in the radial direction if the forces acting on it overcome the friction force at the secondary seal face. In axial direction the FR is pressed by fluid forces and a preload spring against its secondary seal face (see Figure 8). The possibility to move in radial direction is an advantage of FR seals since the rotor is less prone to come into contact with the seal surface. This is especially desirable for LOX Turbopumps, where housing contact will almost certainly lead to oxygen fire and loss of hardware (see section 1.).

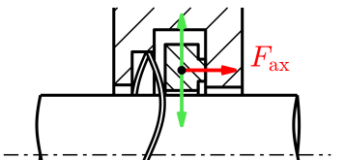

Figure 8. Schematic of a floating ring seal preloaded by a spring. The seal can move in radial direction (green arrows).

The movement of the ring, the friction on the secondary seal face and the mass of the seal ring lead to a different rotordynamic behaviour than the straight gap seal investigated in the previous sections.

According to [4] the fluid forces acting on the rotor can be described by the following equation which is based on equation 2. Since the FR is moving, the acceleration, velocity and position of the shaft are expressed in relative coordinates (e.g. $\ddot{x}_S - \ddot{x}_{fr}$).

$$-\begin{bmatrix} F_x \\ F_y \end{bmatrix} = \begin{bmatrix} M & M_{kk} \\ -M_{kk} & M \end{bmatrix} \begin{bmatrix} \ddot{x}_S - \ddot{x}_{fr} \\ \ddot{y}_S - \ddot{y}_{fr} \end{bmatrix} + \begin{bmatrix} D & D_{kk} \\ -D_{kk} & D \end{bmatrix} \begin{bmatrix} \dot{x}_S - \dot{x}_{fr} \\ \dot{y}_S - \dot{y}_{fr} \end{bmatrix} + \begin{bmatrix} K & K_{kk} \\ -K_{kk} & K \end{bmatrix} \begin{bmatrix} x_S - x_{fr} \\ y_S - y_{fr} \end{bmatrix}$$

$$= \begin{bmatrix} \frac{\dot{x}_{fr}}{|\dot{x}_{fr}|} & 0 \\ 0 & \frac{\dot{y}_{fr}}{|\dot{y}_{fr}|} \end{bmatrix} \begin{bmatrix} \left|\cos\left(\arctan\left(\frac{\dot{y}_{fr}}{\dot{x}_{fr}}\right)\right)\right| \\ \left|\sin\left(\arctan\left(\frac{\dot{y}_{fr}}{\dot{x}_{fr}}\right)\right)\right| \end{bmatrix} \cdot \mu \cdot F_{ax} + \begin{bmatrix} m_{fr} & 0 \\ 0 & m_{fr} \end{bmatrix} \begin{bmatrix} \ddot{x}_{fr} \\ \ddot{y}_{fr} \end{bmatrix} \tag{5}$$

Here index *S* refers to the shaft and index *fr* to the floating ring. F_{ax} is the axial force acting on the FR, μ the friction coefficient on the secondary seal face and m_{fr} is the floating ring mass.

Equation 5 is solved numerically. The rotor dynamic coefficients of the reference geometry are used in the left hand side. F_{ax}, m_{fr} and the eccentricity ϵ are varied, while the friction coefficient is kept constant at $\mu = 0.1$.

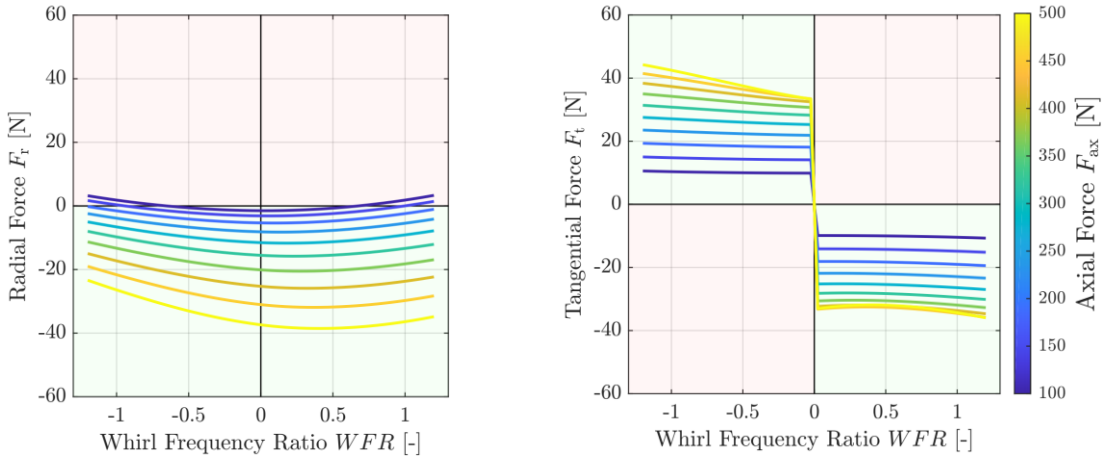

a) radial force **b)** tangential force

Figure 9. effect of axial force F_{ax} on rotor forces of a floating ring seal with $\epsilon = 5\mu m$ and $m_{fr} = 0.1kg$

7.1. Variation of axial force

Figure 9 shows the results of simulations with a constant eccentricity $\epsilon = 5\mu m$ and a constant mass of $m_{fr} = 0.1kg$ for various F_{ax}. For high absolute values of WFR and low axial force there is an unbalance effect on the rotor as the radial force becomes positive. For higher axial force the radial force becomes more and more negative and hence the damping effect on the rotor increases.

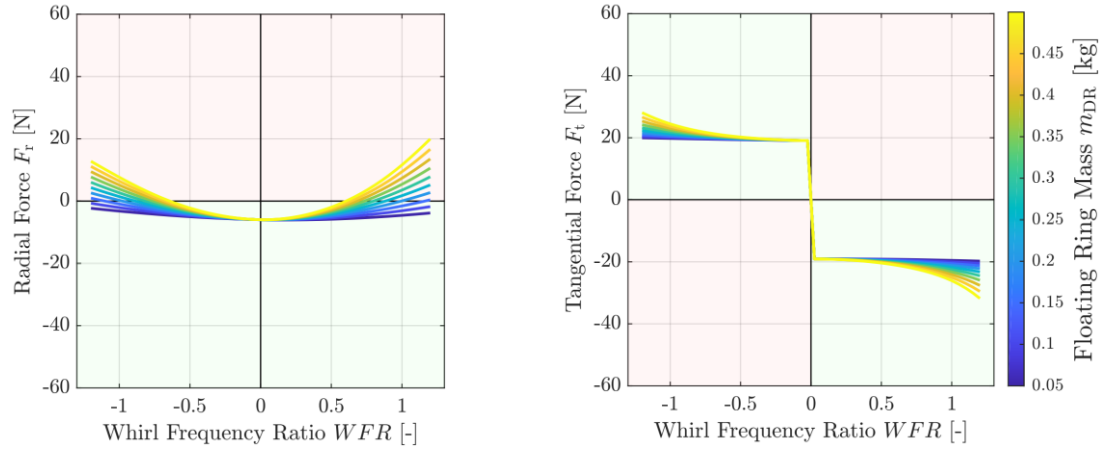

a) radial force **b)** tangential force

Figure 10. effect of floating ring mass m_{fr} on rotor forces of a floating ring seal with $\epsilon = 5\mu m$ and $F_{ax} = 200N$

The tangential forces are always beneficial for rotor dynamics and increase with an increasing axial force.

The increase in radial and tangential force is easily explained by the increase in the friction force on the secondary seal face. Bigger friction forces lead to a larger relative deflection between the rotor and the FR, thus increasing the fluid forces acting on the rotor.

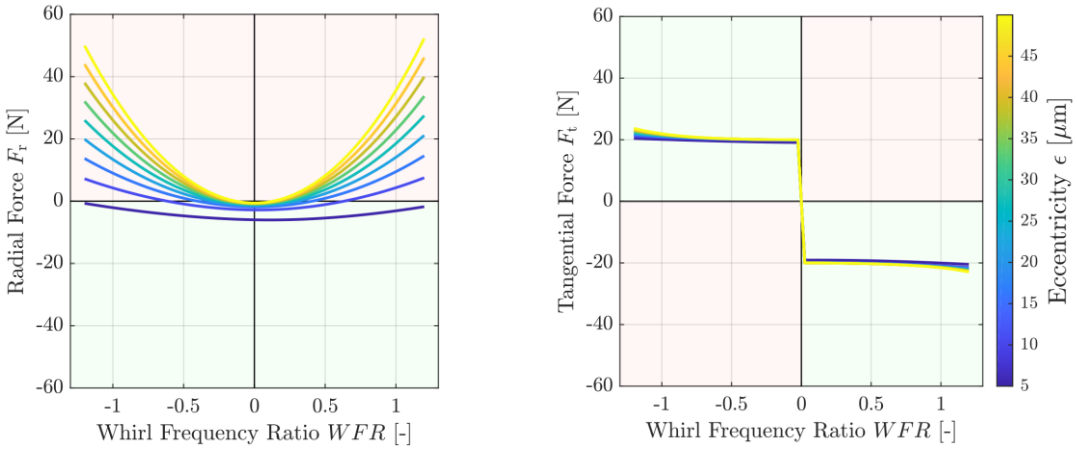

a) radial force **b)** tangential force

Figure 11. effect of eccentricity ϵ on rotor forces of a floating ring seal with $m_{fr} = 0.1kg$ and $F_{ax} = 200N$

7.2. Variation of floating ring mass

Figure 10 shows the results of simulations with a constant eccentricity $\epsilon = 5\mu m$ and a constant axial force of $F_{ax} = 200N$ for various m_{fr}. With increasing FR mass the radial force becomes positive. Higher centrifugal forces are acting on heavier FR so unbalance coupling is increased. The effect on the tangential forces is not very pronounced.

7.3. Variation of eccentricity

A variation of eccentricity from 5µm to 50µm leads to a significant unbalance effect on the rotor and the radial forces (see Figure 11). On the other hand there is almost no influence of the eccentricity on the tangential forces. In this case it is obvious that the axial force should be chosen higher for a real application.

8. Conclusion

In this work we developed a framework to determine the rotor dynamic coefficients of arbitrary seal forms and rotor to housing clearances.

The framework was tested with straight gap seals and is easily used with other seal geometries like labyrinth seals for example. It can even be used for entire pump setups as was shown by the simulation of the rotor to housing clearance. The comparison of two different rotor to housing clearances showed that small clearances can lead to a destabilization of the rotor.

The effect of swirl brakes in the latter has been investigated. The benefits from swirl brakes are evident and the ease of use makes them an almost compulsory design element.

Finally floating ring seals were investigated and a parameter study was carried out. The ring mass, eccentricity and axial force were varied to understand the effect on the rotor force. Floating ring seals have advantages in preventing contact between the rotor and the seal and in having always damping tangential forces. The floating ring properties have to be chosen carefully to ensure that the advantages can be used to their full extend.

References

[1] Traudt, T.; Waxenegger-Wilfing, G.; dos Santos Hahn, R.; Wagner, B. & Deeken, J., An overview on the turbopump Roadmap for the Lumen Demonstrator engine and on the new turbine test facility, *International Aeronautical Congress, Adelaide*, Australia, 2017
[2] Cannon, J.L.: Liquid Propulsion: Propellant Feed System Design, *Encyclopedia of Aerospace Engineering*, Bd. 2 Propulsion & Power, Wiley, 2010
[3] NASA, Orb–3 Accident Investigation Report, 2015
[4] Tokunaga, Y.; Inoue, H.; Hiromatsu, J.; Iguchi, T.; Kuroki, Y.; Uchiumi, M., Rotordynamic Characteristics of Floating Ring Seals in Rocket Turbopumps, *International Journal of Fluid Machinery and Systems*, Korean Fluid Machinery Association, 2016, 9, 194-204
[5] Gasch, R.; Nordmann, R.; Pfützner, H.: *Rotordynamik*, 2. Aufl., Springer, 2006
[6] Staubli, T.; Bissig, M.: Numerically calculated rotor dynamic coefficients of a pump rotor side space, *International Symposium on Stability Control of Rotating Machinery*, 2001
[7] Max Axel Müller; Numerical calculation of the Rotordynamic Coefficients of a LOX-Turbopump Seal, *University of Stuttgart*, 2019
[8] Childs, D. W., Dynamic Analysis of Turbulent Annular Seals Based On Hirs' Lubrication Equation, Journal of Lubrication Technology, ASME International, 1983, 105, 429-436
[9] ANSYS®, "CFX," 18.2
[10] Lomakin, A.A.: Calculation of Critical Speeds and Securing of Dynamic Stability of Hydraulic High-Pressure Machines with reference of the Forces Arising in the Gap Seals, *Energomashinotroenie*, 4, 1958